IAEA
International Atomic Energy Agency

INDC(EUR)-0036
Distr. G+J

INDC International Nuclear Data Committee

Results of time-of-flight transmission measurements for ^{nat}Ag at a 10 m station of GELINA

L. Šalamon[a,b], J. Heyse[b], C. Paradela[b], G.Alaerts[b], S. Kopecky[b], G. Noguere[a], P. Schillebeeckx[b], R. Wynants[b] and L. Snoj[c]

[a] DER, DEN, CEA, Cadarache, Saint-Paul-lez-Durance, France
[b] European Commission, Joint Research Centre, Geel, Belgium
[c] Reactor Physics Division, Jozef Stefan Institute, Ljubljana, Slovenia

March 2020

IAEA Nuclear Data Section, Vienna International Centre, A-1400 Vienna, Austria

Selected INDC documents may be downloaded in electronic form from
http://www-nds.iaea.org/publications/
or sent as an e-mail attachment.
Requests for hardcopy or e-mail transmittal should be directed to
nds.contact-point@iaea.org
or to:

Nuclear Data Section
International Atomic Energy Agency
Vienna International Centre
PO Box 100
A-1400 Vienna
Austria

Produced by the IAEA in Austria
March 2020

INDC(EUR)-0036
Distr. G+J

Results of time-of-flight transmission measurements for ^{nat}Ag at a 10 m station of GELINA

L. Šalamon[a,b], J. Heyse[b], C. Paradela[b], G.Alaerts[b], S. Kopecky[b], G. Noguere[a], P. Schillebeeckx[b], R. Wynants[b] and L. Snoj[c]

[a] DER, DEN, CEA, Cadarache, Saint-Paul-lez-Durance, France
[b] European Commission, Joint Research Centre, Geel, Belgium
[c] Reactor Physics Division, Jozef Stefan Institute, Ljubljana, Slovenia

March 2020

Results of time-of-flight transmission measurements for ^{nat}Ag at a 10 m station of GELINA

L. Šalamon[a,b], J. Heyse[b], C. Paradela[b], G.Alaerts[b], S. Kopecky[b], G. Noguere[a], P. Schillebeeckx[b], R. Wynants[b] and L. Snoj[c]

[a]DER, DEN, CEA, Cadarache, F-13108 Saint-Paul-lez-Durance, France
[b]European Commission, Joint Research Centre, B - 2440 Geel, Belgium
[c]Reactor Physics Division, Jozef Stefan Institute, SI-1000 Ljubljana, Slovenia

Abstract. Transmission measurements have been performed at the time-of-flight facility GELINA to determine neutron resonance parameters for ^{107}Ag and ^{109}Ag. The measurements were carried out at the 10 m transmission station using a Li-glass scintillator with the accelerator operating at 800 Hz. This report provides the experimental details required to deliver the data to the EXFOR data library which is maintained by the International Network of Nuclear Reaction Data Centres (NRDC). The experimental conditions and data reduction procedures are described. In addition, the full covariance information based on the AGS concept is given such that nuclear reaction model parameters together with their covariances can be derived in a least-squares adjustment to the data.

1 Introduction

To study the resonance structure of neutron induced reaction cross sections, neutron spectroscopic measurements are required, which determine with a high accuracy the energy of the neutron that interacts with the material under investigation. To cover a broad energy-range such measurements are best carried out with a pulsed white neutron source, which is optimized for time-of-flight (TOF) measurements [1].

The TOF-facility GELINA [2][3] has been designed and built for high-resolution cross section measurements in the resonance region. It is a multi-user facility, providing a white neutron source with a neutron energy range from 10 meV to 20 MeV. The GELINA facility can host up to 10 experiments at measurement stations located between 10 m and 400 m from the neutron production target. The electron linear accelerator provides a pulsed electron beam with a maximum energy of 150 MeV, a maximum peak current of 10 A and a repetition rate ranging from 50 Hz to 800 Hz. A compression magnet reduces the width

of the electron pulses to about 2 ns [4]. The electron beam hits a mercury-cooled uranium target producing Bremsstrahlung and subsequently neutrons via photonuclear reactions [5]. Two water-filled beryllium containers mounted above and below the neutron production target are used to moderate the neutrons. By applying different neutron beam collimation conditions, experiments can use either a fast or a moderated neutron spectrum. The neutron production rate is monitored by BF_3 proportional counters which are mounted in the ceiling of the target hall. The output of the monitors is used to normalize the time-of-flight spectra to the same neutron intensity. The measurement stations are equipped with air conditioning systems that maintain a constant temperature to reduce electronic drifts in the detection chains due to temperature changes.

This report describes the transmission measurements carried out at GELINA with ^{nat}Ag, composed of ^{107}Ag (51.8 wt%) and ^{109}Ag (49.2 wt%), metallic samples. To reduce bias effects due to e.g. dead time and background, the measurement and data reduction procedures recommended in Ref. [1]. have been followed. The report provides the information required for extracting ^{107}Ag and ^{109}Ag resonance parameters by using the resonance shape analysis code REFIT [6]. In the description of the data the recommendations resulting from a consultant's meeting organized by the Nuclear Data Section of the IAEA (NDS/IAEA) have been followed [7].

2 Experimental conditions

The transmission experiments were performed at the 10 m measurement station of flight path 13 with the accelerator operating at 800 Hz. The moderated neutron spectrum was used. A shadow bar made of Cu and Pb was placed close to the uranium target to reduce the intensity of the γ-ray flash and the fast neutron component. The flight path forms an angle of 18° with the direction normal to the face of the moderator viewing the flight path. The samples and detector were placed in a acclimatized room to keep them at a constant temperature of 20 °C.

The partially thermalized neutrons scattered from the moderators were collimated into the flight path through an evacuated aluminium pipe of 50 cm diameter with annular collimators, consisting of borated wax, copper and lead. A set of Pb, Ni and Cu annular collimators was used to reduce the neutron beam to a diameter of 10 mm at the sample position. Additional lithium and B_4C collimators were installed to absorb neutrons that are scattered by the collimators [8]. Either ^{10}B or Cd overlap filters were used to minimize the contribution of slow neutrons coming from previous accelerator bursts and a Pb filter to reduce the impact of the γ-ray flash in the neutron detector. In addition, permanent Na and Co black resonance filters were used to continuously monitor the background level at 2850 eV and 132 eV, respectively, and to account for the impact of the sample or other filters placed in the beam [1]. Additional measurements with Rh, Ag and W black resonance filters were carried out for a complete characterization of the background time dependence. The samples and these additional filters were placed at 7.7 m distance from the neutron source. The neutron beam passing through the sample and filters was further collimated and detected by a 6.35 mm x 76 mm x 76 mm Scionix Li-glass scintillator. The detector was placed at about 11 m from the neutron target.

The TOF of the detected neutron was derived from the time difference between the stop signal T_s, obtained from the anode pulse of the PMT, and the start signal T_0, given at each electron burst. This time difference was processed with a multi-hit fast time coder with a 1 ns time resolution. The TOF and the pulse height of each detected event were recorded in list mode using a multi-parameter data acquisition system developed at the JRC Geel [9]. Each measurement was subdivided in different cycles. Only cycles for which the ratio between the total counts in the transmission detector and in the neutron monitor deviated by less than 1 % were selected. The dead time of the detection chain t_d = 3024 (10) ns was derived from a spectrum of the time-interval between successive events. The

uncertainties due to dead time corrections in the region of interest are very small and can be neglected.

All measurements were performed with natural Ag metallic discs of different thicknesses and a diameter of 80 mm. The main characteristics of the samples are reported in Table 1. The areal density of the samples was derived from a measurement of the weight and the area with an uncertainty better than 0.1 %. The mass was determined by substitution weighing with a microbalance from Mettler Toledo. The area was determined by an optical surface inspection with a microscope system from Mitutoyo [10].

Table 1 Characteristics of the samples used for the transmission measurements. Each areal density n_d was calculated by using the experimentally determined mass and area.

ID	Thickness /mm	Mass/g	Area/mm2	Areal Density (at/b)
1	0.126	6.6366 (1)	50.3088 (3)	7.3646 (1) x 10^{-4}
2	0.06	3.4056 (1)	50.2376 (89)	3.7845 (8) x 10^{-4}

3 Data reduction

The AGS code [12][13], developed at the JRC Geel, was used to derive the experimental transmission from the TOF-spectra. The code is based on a compact formalism to propagate all uncertainties starting from uncorrelated uncertainties due to counting statistics.

3.1 Experimental transmission

The experimental transmission T_{exp} as a function of TOF was obtained from the ratio of a sample-in measurement C_{in} and a sample-out measurement C_{out}, both corrected for their background contributions B_{in} and B_{out}, respectively:

$$T_{exp} = N\frac{C_{in} - KB_{in}}{C_{out} - KB_{out}}. \quad (3.1)$$

The TOF spectra, C_{in} and C_{out}, were corrected for losses due to the dead time in the detector and electronics chain. All spectra were normalized to the same TOF-bin width structure and neutron beam intensity. The latter was derived from the response of the BF_3 beam monitors. To avoid systematic effects due to slow variations of both the beam intensity and detector efficiency as a function of time, data were taken by alternating sample-in and sample-out measurements in cycles of about 600 seconds. Such a procedure reduces the uncertainty on the normalization to the beam intensity to less than 0.25 %. This uncertainty was evaluated from the ratios of counts in the ^{6}Li transmission detector and in the flux monitors. To account for this uncertainty the factor N= 1.0000 (25) was introduced in Eq. (3.1). The background as a function of TOF was approximated by an analytic expression applying the black resonance technique [1]. The factor K = 1.00 (3) in Eq. (3.1) was introduced to account for systematic effects due to the background model. Its uncertainty was derived from a statistical analysis of the difference between the observed black resonance dips and the estimated background [14]. This uncertainty is only valid for measurements with at least two fixed black resonance filters in the beam [1].

The time-of-flight (t) of a neutron creating a signal in the neutron detector was determined by the time difference between the start signal (T_0) and the stop signal (T_s):

$$t = (T_s - T_0) + t_0, \quad (3.2)$$

with t_0 a time-offset which was determined by a measurement of the γ-ray flash. The flight path distance L = 10.860 (1) m, i.e. the distance between the centre of the moderator

viewing the flight path and the front face of the detector, was derived previously from results of transmission measurements using uranium standard references.

3.2 Background correction

The background as a function of TOF for the measurement with the ^{10}B overlap filter was parameterized by an analytical function:

$$B(t) = b_0 + b_1 e^{-\lambda_1 t} + b_2 e^{-\lambda_2 t} + b_3 e^{-\lambda_3 (t+\tau_0)}. \quad (3.3)$$

It consists of a time independent and three time-dependent exponential terms. The time independent component b_0 is related to the ambient radiation and background contributions that lost any time correlation. The first time-dependent component is due to 2.2 MeV γ-rays resulting from neutron capture in hydrogen present in the moderator, the second exponential term is due to neutrons scattered inside the detector station and neutrons scattered at other flight paths, and the last one originates from slow neutrons coming from previous accelerator pulses. The decay constants λ_1 and λ_2 were derived from transmission data measured with additional black resonance filters (Rh, Ag and W), while λ_3 was obtained by extrapolating the TOF spectra behavior at large times, i.e. for $t > 8 \times 10^5$ ns. The parameter τ_0 is related to the operating frequency of accelerator (τ_0 =1.25 ms for 800 Hz). This extrapolation applied to each measurement also provides the amplitudes b_0 and b_3, whereas the amplitudes b_1 and b_2 were adjusted by using the black resonance dips of the permanent filters (Co and Na) [11]. Example of a dead-time corrected and normalized sample-in spectrum with the background contributions from Eq. (3.3) are shown in Figure 1.

Figure 1. TOF spectrum with the 0.126 mm thick Ag metallic disc sample (C_{in}) and the ^{10}B overlap filter in the beam at 800 Hz together with the total background (B_{in}) and its different components as given in Eq. (3.3).

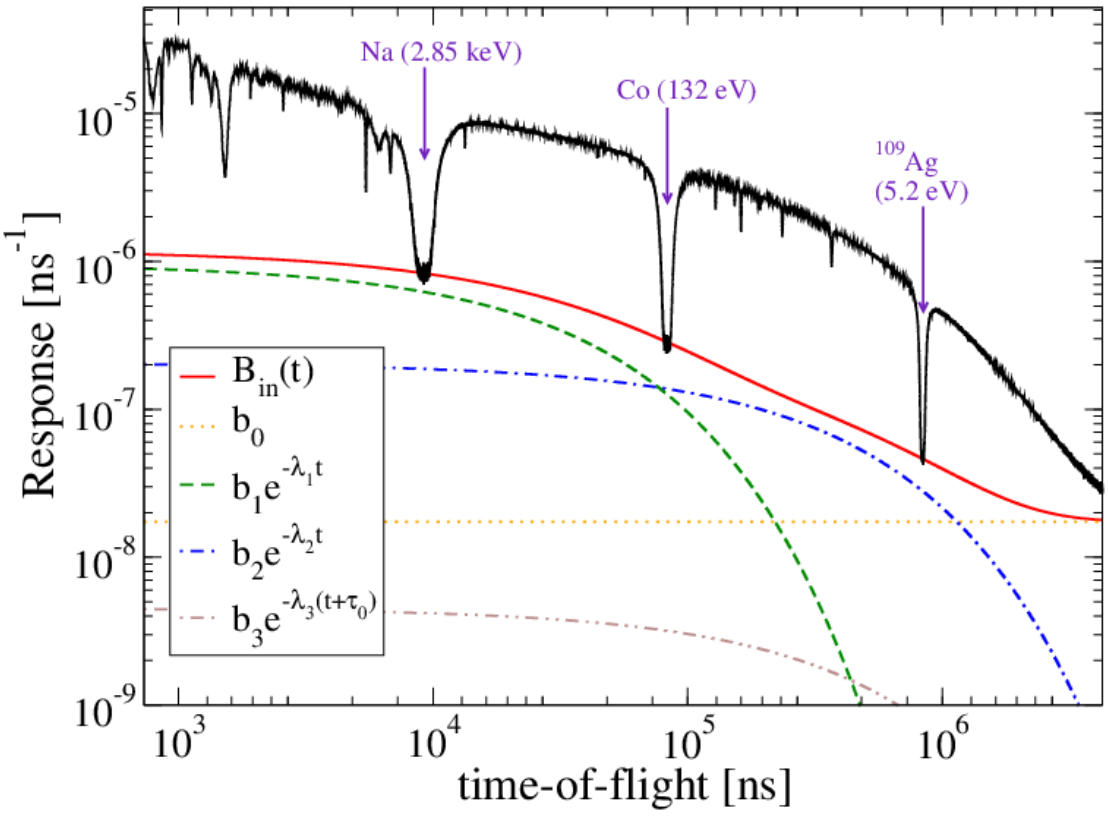

For the parameterization of the background with the Cd overlap filter, it is assumed that all neutrons below the cadmium cut-off energy at around 0.5 eV are absorbed and for this reason the overlap component is neglected. The background for these measurements was approximated by Eq. (3.4):

$$B(t) = b_0 + b_1 e^{-\lambda_1 t} + b_2 e^{-\lambda_2 t}. \quad (3.4)$$

The decay constant λ_1, due to the γ-ray background, was supposed to be the same as for the measurements with the ^{10}B filter. The decay constant λ_2 was derived from measurements with additional black resonance filters. The amplitudes b_0, b_1 and b_2 were adjusted for each measurement by using the black resonance dips due to the presence of the Cd, Co and Na filters.

Table 2. Parameters for the analytical expressions of the background correction for the sample-in and sample-out measurements for the natural silver sample of 0.126 mm measured at the 800 Hz linac frequency using the ^{10}B overlap filter.

ID	$b_0/10^{-8}$ ns^{-1}	$b_1/10^{-7}$ ns^{-1}	$\lambda_1/10^{-5}$ ns^{-1}	$b_2/10^{-7}$ ns^{-1}	$\lambda_2/10^{-6}$ ns^{-1}	$b_3/10^{-6}$ ns^{-1}	$\lambda_3/10^{-6}$ ns^{-1}
B_{in}	1.74	9.62	-2.96	2.04	-5.76	2.72	5.12
B_{out}	1.74	9.56	-2.96	2.04	-5.76	2.72	5.12

Table 3. Parameters for the analytical expressions of the background correction for the sample-in and sample-out measurements for the natural silver sample of 0.126 mm measured at the 800 Hz linac frequency using the Cd overlap filter.

ID	$b_0/10^{-8}$ ns^{-1}	$b_1/10^{-6}$ ns^{-1}	$\lambda_1/10^{-5}$ ns^{-1}	$b_2/10^{-7}$ ns^{-1}	$\lambda_2/10^{-6}$ ns^{-1}
B_{in}	1.74	1.02	-2.96	1.93	-4.13
B_{out}	1.74	1.02	-2.96	1.93	-4.13

Table 4. Parameters for the analytical expressions of the background correction for the sample-in and sample-out measurements for the natural silver sample of 0.06 mm measured at the 800 Hz linac frequency using the ^{10}B overlap filter.

ID	$b_0/10^{-8}$ ns^{-1}	$b_1/10^{-7}$ ns^{-1}	$\lambda_1/10^{-5}$ ns^{-1}	$b_2/10^{-7}$ ns^{-1}	$\lambda_2/10^{-6}$ ns^{-1}	$b_3/10^{-6}$ ns^{-1}	$\lambda_3/10^{-6}$ ns^{-1}
B_{in}	1.78	9.74	-2.96	2.02	-5.50	2.76	5.12
B_{out}	1.78	9.74	-2.96	2.02	-5.50	2.79	5.12

Table 5. Parameters for the analytical expressions of the background correction for the sample-in and sample-out measurements for the natural silver sample of 0.06 mm measured at the 800 Hz linac frequency using the Cd overlap filter.

ID	$b_0/10^{-8}$ ns^{-1}	$b_1/10^{-7}$ ns^{-1}	$\lambda_1/10^{-5}$ ns^{-1}	$b_2/10^{-7}$ ns^{-1}	$\lambda_2/10^{-6}$ ns^{-1}
B_{in}	2.41	9.81	-2.96	2.03	-3.92
B_{out}	2.41	9.81	-2.96	2.03	-3.92

4 Results

The AGS code [12][13] was used to derive the experimental transmission and propagate both the correlated and uncorrelated uncertainties. The code is based on a compact formalism to propagate all uncertainties starting from uncorrelated uncertainties due to counting statistics. It stores the full covariance information after each operation in a concise, vectorized way. The AGS formalism results in a substantial reduction of data storage volume and provides a convenient structure to verify the various sources of uncertainties through each step of the data reduction process. The concept is recommended by the NDS/IAEA [7] to prepare the experimental observables, including their full covariance information, for storage into the EXFOR data library [15][16].

Figure 2. Experimental transmission as a function of time-of-flight resulting from measurements with the 0.126 mm thick ^{nat}Ag sample at 800 Hz in the energy region 12.0-20.0 eV compared with the transmission spectrum calculated with REFIT by using resonance parameters provided in the JEFF-3.0 evaluation.

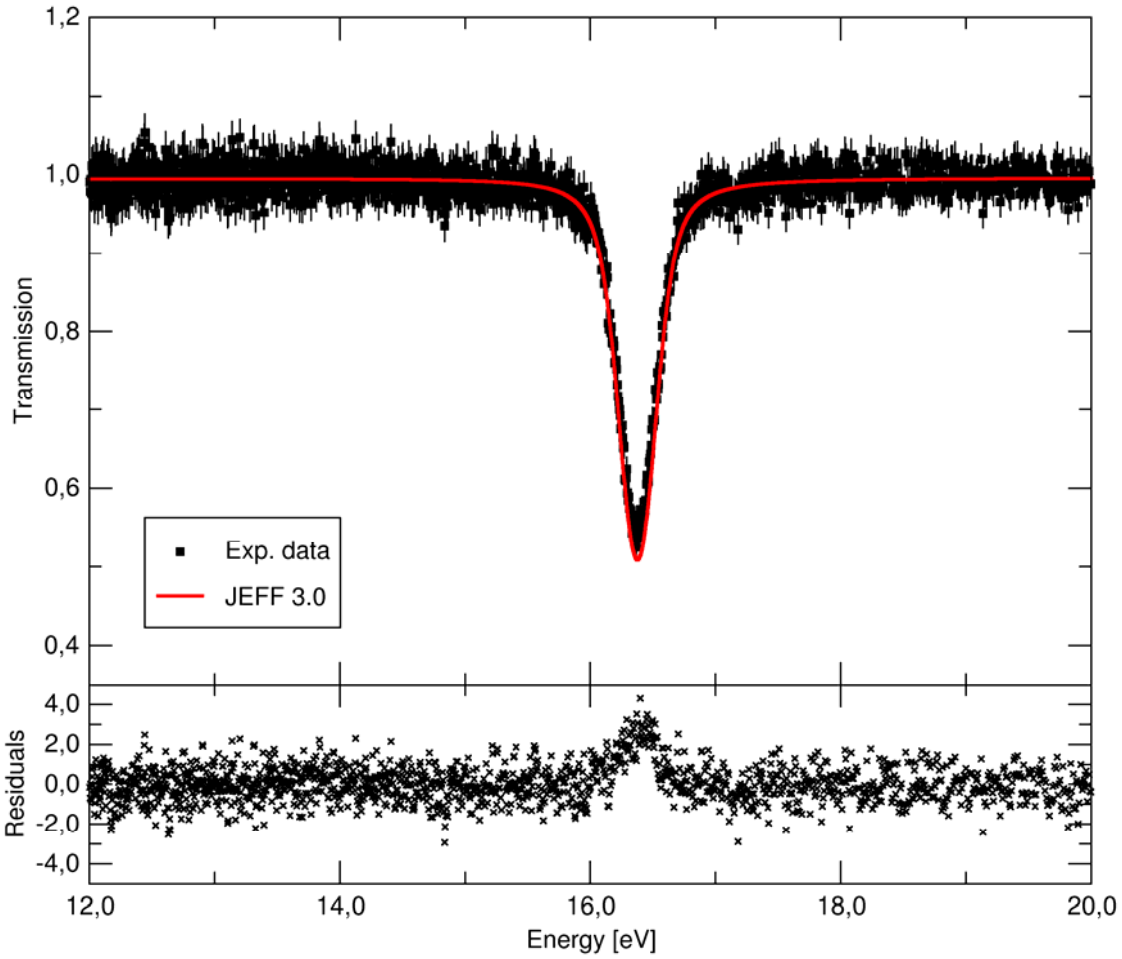

The experimental transmission resulting from the measurement with the 0.126 mm thick ^{nat}Ag sample is shown in Figure 2. The experimental transmission is compared with the transmission calculated with the resonance parameters in the JEFF-3.0 evaluation library. In order to obtain the theoretical transmission, the following expression is implemented in the REFIT code:

$$T_M(t) = \int R(t,E) e^{-n\sigma_{tot}(E)} dE. \quad (4.1)$$

The response function of the TOF spectrometer, R(t,E), represents the probability that a neutron with energy E is detected with a time-of-flight t. The response function can be considered as the convolution of the duration of the accelerator burst, the time resolution of the detection system and the neutron transport in the neutron target and in the detector [1][17]. The residuals in the figure indicate that the evaluated resonance parameters can be improved.

The format in which the numerical data will be stored in the EXFOR data library is illustrated in the Appendix. The data include the full covariance information based on the AGS concept. The total uncertainty and the uncertainty due to uncorrelated components are reported, together with the contributions due to the normalization and background subtraction. Applying the AGS concept the covariance matrix V of the experimental transmission can be calculated by:

$$V = U_u + S(\eta)S(\eta)^T, \tag{4.2}$$

where U_u is a diagonal matrix containing the contribution of all uncorrelated uncertainty components. The matrix S contains the contribution of the components $\eta = \{N, K\}$ creating correlated components. The uncertainty due to the dead time correction can be neglected. The experimental details, which are required to perform a resonance analysis on the data, are summarized in the Appendix.

Acknowledgements

This work was supported by the EUFRAT open access programme of the Joint Research Centre.

References

[1] P. Schillebeeckx, B. Becker,Y. Danon, K. Guber, H. Harada, J. Heyse, A.R. Junghans, S. Kopecky, C. Massimi, M.C. Moxon, N. Otuka, I. Sirakov and K. Volev, "Determination of resonance parameters and their covariances from neutron induced reaction cross section data", Nucl. Data Sheets 113 (2012) 3054 – 3100.

[2] A. Bensussan and J.M. Salomé, "GELINA: A modern accelerator for high resolution neutron time of flight experiments", Nucl. Instr. Meth. 155 (1978) 11 – 23.

[3] W. Mondelaers and P. Schillebeeckx, "GELINA, a neutron time-of-flight facility for neutron data measurements", Notiziario Neutroni e Luce di Sincrotrone 11 (2006) 19 – 25.

[4] D. Tronc, J.M. Salomé and K.H. Böckhoff, "A new pulse compression system for intense relativistic electron beams", Nucl. Instr. Meth. 228 (1985) 217 – 227.

[5] J.M. Salome and R. Cools, "Neutron producing targets at GELINA", Nucl. Instr. Meth. 179 (1981) 13 – 19.

[6] M.C. Moxon and J.B. Brisland, Technical Report AEA-INTEC-0630, AEA Technology (1991).

[7] F. Gunsing, P. Schillebeeeckx and V. Semkova, Summary Report of the Consultants' Meeting on EXFOR Data in Resonance Region and Spectrometer Response Function, IAEA Headquarters, Vienna, Austria, 8-10 October 2013, INDC(NDS)-0647 (2013), https://www-nds.iaea.org/index-meeting-crp/CM-RF-2013/ (03/05/2016).

[8] C. Paradela et al. "Neutron resonance analysis for nuclear safeguards and security applications", EPJ Web of Conferences. Vol. 146. EDP Sciences, 2017.

[9] J. Gonzalez, C. Bastian, S. de Jonge, and K. Hofmans, "Modular Multi-Parameter Multiplexer MMPM. Hardware description and user guide", Internal Report GE/R/INF/06/97, IRMM, Geel.

[10] https://www.mitutoyo.co.jp/eng/ (03/06/2016).

[11] L. Šalamon, B. Geslot, J. Heyse, S. Kopecky, P. Leconte, G. Noguere, C. Paradela, P. Schillebeeckx and L. Snoj, "^{107}Ag and ^{109}Ag resonance parameters for neutron induced reactions below 1 keV", Nuclear Inst. Meth. B 446 (2019) 19-28.

[12] B. Becker, C. Bastian, J. Heyse, S. Kopecky and P. Schillebeeckx, "AGS – Analysis of Geel Spectra User's Manual", NEA/DB/DOC(2014)4.

[13] B. Becker, C. Bastian, F. Emiliani, F. Gunsing, J. Heyse, K. Kauwenberghs, S. Kopecky, C. Lampoudis, C. Massimi, N. Otuka, P. Schillebeeckx and I. Sirakov, "Data reduction and uncertainty propagation of time-of-flight spectra with AGS", J. of Instrumentation, 7 (2012) P11002 – 19.

[14] I. Sirakov, B. Becker, R. Capote, E. Dupont, S. Kopecky, C. Massimi, and P. Schillebeeckx, "Results of total cross section measurements for ^{197}Au in the neutron energy region from 4 to 108 keV at GELINA", Eur. Phys. J. A 49 (144) (2013) 1.

[15] N. Otuka et al., "Towards a More Complete and Accurate Experimental Nuclear Reacton Data Library (EXFOR): International Collaboration Between Nuclear Reaction Data Centres (NRDC)", Nucl. Data Sheets 120 (2014) 272-276.

[16] N. Otuka, A. Borella, S. Kopecky, C. Lampoudis, and P. Schillebeeckx, "Database for time-of-flight spectra with their covariances", J. Korean Phys. Soc. 59 (2011) 1314 – 1317.

[17] M. Flaska, A. Borella, D. Lathouwers, L.C. Mihailescu, W. Mondelaers, A.J.M. Plompen, H. van Dam and T.H.J.J. van der Hagen, "Modeling of the GELINA neutron target using coupled electron–photon–neutron transport with the MCNP4C3 code", Nucl. Instr. Meth. A 531 (2004) 392–406.

Appendix

A. SUMMARY OF EXPERIMENTAL DETAILS

A. 1 Experiment description (ID 1)

1. Main Reference		[a]
2. Facility	GELINA	[b]
3. Neutron production		
Neutron production beam	Electron	
Nominal average beam energy	100 MeV	
Nominal average current	50 μA	
Repetition rate (pulses per second)	800 Hz	
Pulse width	2 ns	
Primary neutron production target	Mercury cooled depleted uranium	
Target nominal neutron production intensity	3.4 x10^{13} s^{-1}	
4. Moderator		
Primary neutron source position in moderator	Above and below uranium target	
Moderator material	2 water filled Be-containers around U-target	
Moderator dimensions (internal)	2 x (14.6 cm x 21 cm x 3.9 cm)	
Density (moderator material)	1 g/cm^3	
Temperature (K)	Room temperature	
Moderator-room decoupler (Cd, B, …)	None	
5. Other experimental details		
Measurement type	Transmission	
Method (total energy, total absorption, …)	Good transmission geometry	[c][d]
Flight Path length (m) (moderator centre-detector front face)	L = 10.860 (1) m	
Flight path direction	18° with respect to normal of the moderator face viewing the flight path	
Neutron beam dimensions at sample position	10 mm in diameter	
Neutron beam profile	-	
Overlap suppression	^{10}B overlap filter	
Other fixed beam filters	Na, Co, Pb	
6. Detector		
Type	Scintillator	
Material	Li-glass	
Surface Dimensions	76 mm x 76 mm square	
Thickness (cm)	6.35 mm	
Detector(s) position relative to neutron beam	In the beam	
Detector(s) solid angle	-	
Sample		
7. Type (metal, powder, liquid, crystal)	Metal	
Chemical composition	^{nat}Ag (100 at %)	
Sample composition (at/b)	7.3646 (1) x 10^{-4} at/b	
Temperature	20 ℃	
Sample mass (g)	6.6366 (1) g	
Geometrical shape (cylinder, sphere, …)	Cylinder	

Surface dimension	50.3088 (3) mm^2	
Nominal thickness (mm)	0.126 mm	
Containment description	None	
Data Reduction Procedure		[d][e]
8. Dead time correction	Done (< factor 1.05)	
Back ground subtraction	Black resonance technique	
Flux determination (reference reaction, …)	-	
Normalization	1.0000 (25)	
Detector efficiency	-	
Self-shielding	-	
Time-of-flight binning	Zone length bin width 10240 2 ns 4096 4 ns 4096 8 ns 4096 16 ns 4096 32 ns 4096 64 ns 6144 128 ns 28672 64 ns	
Response function		
9. Initial pulse	Normal distribution, FWHM = 2 ns	
Target / moderator assembly	Numerical distribution from MC simulations	[f][g]
Detector	Analytical function defined in REFIT manual	[h]

A. 2 Experiment description (ID 2)

1. Main Reference		[a]
2. Facility	GELINA	[b]
3. Neutron production		
Neutron production beam	Electron	
Nominal average beam energy	100 MeV	
Nominal average current	50 μA	
Repetition rate (pulses per second)	800 Hz	
Pulse width	2 ns	
Primary neutron production target	Mercury cooled depleted uranium	
Target nominal neutron production intensity	3.4 x10^{13} s^{-1}	
4. Moderator		
Primary neutron source position in moderator	Above and below uranium target	
Moderator material	2 water filled Be-containers around U-target	
Moderator dimensions (internal)	2 x (14.6 cm x 21 cm x 3.9 cm)	
Density (moderator material)	1 g/cm^3	
Temperature (K)	Room temperature	
Moderator-room decoupler (Cd, B, …)	None	
5. Other experimental details		
Measurement type	Transmission	

	Method (total energy, total absorption, …)	Good transmission geometry	[c][d]
	Flight Path length (m) (moderator centre-detector front face)	L = 10.860 (1) m	
	Flight path direction	18° with respect to normal of the moderator face viewing the flight path	
	Neutron beam dimensions at sample position	10 mm in diameter	
	Neutron beam profile	-	
	Overlap suppression	5 mm Cd overlap filter	
	Other fixed beam filters	Na, Co, Pb	
6.	**Detector**		
	Type	Scintillator	
	Material	Li-glass	
	Surface Dimensions	76 mm x 76 mm square	
	Thickness (cm)	6.35 mm	
	Detector(s) position relative to neutron beam	In the beam	
	Detector(s) solid angle	-	
	Sample		
7.	Type (metal, powder, liquid, crystal)	Metal	
	Chemical composition	^{nat}Ag (100 at %)	
	Sample composition (at/b)	7.3646 (1) x 10^{-4} at/b	
	Temperature	20 ℃	
	Sample mass (g)	6.6366 (1) g	
	Geometrical shape (cylinder, sphere, …)	Cylinder	
	Surface dimension	50.3088 (3) mm^2	
	Nominal thickness (mm)	0.126 mm	
	Containment description	None	
Data Reduction Procedure			[d][e]
8.	Dead time correction	Done (< factor 1.05)	
	Back ground subtraction	Black resonance technique	
	Flux determination (reference reaction, …)	-	
	Normalization	1.0000 (25)	
	Detector efficiency	-	
	Self-shielding	-	
	Time-of-flight binning	Zone length bin width 10240 2 ns 4096 4 ns 4096 8 ns 4096 16 ns 4096 32 ns 4096 64 ns 6144 128 ns 28672 64 ns	
	Response function		
9.	Initial pulse	Normal distribution, FWHM = 2 ns	
	Target / moderator assembly	Numerical distribution from MC simulations	[f][g]
	Detector	Analytical function defined in REFIT manual	[h]

A. 3 Experiment description (ID 3)

1. Main Reference		[a]
2. Facility	GELINA	[b]
3. Neutron production		
Neutron production beam	Electron	
Nominal average beam energy	100 MeV	
Nominal average current	50 μA	
Repetition rate (pulses per second)	800 Hz	
Pulse width	2 ns	
Primary neutron production target	Mercury cooled depleted uranium	
Target nominal neutron production intensity	3.4 x10^{13} s^{-1}	
4. Moderator		
Primary neutron source position in moderator	Above and below uranium target	
Moderator material	2 water filled Be-containers around U-target	
Moderator dimensions (internal)	2 x (14.6 cm x 21 cm x 3.9 cm)	
Density (moderator material)	1 g/cm^3	
Temperature (K)	Room temperature	
Moderator-room decoupler (Cd, B, …)	None	
5. Other experimental details		
Measurement type	Transmission	
Method (total energy, total absorption, …)	Good transmission geometry	[c][d]
Flight Path length (m) (moderator centre-detector front face)	L = 10.860 (1) m	
Flight path direction	18° with respect to normal of the moderator face viewing the flight path	
Neutron beam dimensions at sample position	10 mm in diameter	
Neutron beam profile	-	
Overlap suppression	^{10}B overlap filter	
Other fixed beam filters	Na, Co, Pb	
6. Detector		
Type	Scintillator	
Material	Li-glass	
Surface Dimensions	76 mm x 76 mm square	
Thickness (cm)	6.35 mm	
Detector(s) position relative to neutron beam	In the beam	
Detector(s) solid angle	-	
7. Sample		
Type (metal, powder, liquid, crystal)	Metal	
Chemical composition	^{nat}Ag (100 at %)	
Sample composition (at/b)	3.7845 (8) x 10^{-4}at/b	
Temperature	19 ℃	
Sample mass (g)	3.4056 (1) g	
Geometrical shape (cylinder, sphere, …)	Cylinder	
Surface dimension	50.2376 (89) mm^2	
Nominal thickness (mm)	0.06 mm	
Containment description	None	

8. Data Reduction Procedure		[d][e]
Dead time correction	Done (< factor 1.05)	
Back ground subtraction	Black resonance technique	
Flux determination (reference reaction, …)	-	
Normalization	1.0000 ± 0.0025	
Detector efficiency	-	
Self-shielding	-	
Time-of-flight binning	Zone length bin width 10240 2 ns 4096 4 ns 4096 8 ns 4096 16 ns 4096 32 ns 4096 64 ns 6144 128 ns 28672 64 ns	
9. Response function		
Initial pulse	Normal distribution, FWHM = 2 ns	
Target / moderator assembly	Numerical distribution from MC simulations	[f][g]
Detector	Analytical function defined in REFIT manual	[h]

A. 4 Experiment description (ID 4)

1. Main Reference		[a]
2. Facility	GELINA	[b]
3. Neutron production		
Neutron production beam	Electron	
Nominal average beam energy	100 MeV	
Nominal average current	50 μA	
Repetition rate (pulses per second)	800 Hz	
Pulse width	2 ns	
Primary neutron production target	Mercury cooled depleted uranium	
Target nominal neutron production intensity	3.4 x10^{13} s^{-1}	
4. Moderator		
Primary neutron source position in moderator	Above and below uranium target	
Moderator material	2 water filled Be-containers around U-target	
Moderator dimensions (internal)	2 x (14.6 cm x 21 cm x 3.9 cm)	
Density (moderator material)	1 g/cm^3	
Temperature (K)	Room temperature	
Moderator-room decoupler (Cd, B, …)	None	
5. Other experimental details		
Measurement type	Transmission	
Method (total energy, total absorption, …)	Good transmission geometry	[c][d]
Flight Path length (m) (moderator centre-detector front face)	L = 10.860 (1) m	

	Flight path direction	18° with respect to normal of the moderator face viewing the flight path	
	Neutron beam dimensions at sample position	10 mm in diameter	
	Neutron beam profile	-	
	Overlap suppression	5 mm Cd overlap filter	
	Other fixed beam filters	Na, Co, Pb	
6.	**Detector**		
	Type	Scintillator	
	Material	Li-glass	
	Surface Dimensions	76 mm x 76 mm square	
	Thickness (cm)	6.35 mm	
	Detector(s) position relative to neutron beam	In the beam	
	Detector(s) solid angle	-	
7.	**Sample**		
	Type (metal, powder, liquid, crystal)	Metal	
	Chemical composition	^{nat}Ag (100 at %)	
	Sample composition (at/b)	3.7845 (8) x 10^{-4}at/b	
	Temperature	20 ℃	
	Sample mass (g)	3.4056 (1) g	
	Geometrical shape (cylinder, sphere, …)	Cylinder	
	Surface dimension	50.2376 (89) mm^2	
	Nominal thickness (mm)	0.06 mm	
	Containment description	None	
8.	**Data Reduction Procedure**		[d][e]
	Dead time correction	Done (< factor 1.05)	
	Back ground subtraction	Black resonance technique	
	Flux determination (reference reaction, …)	-	
	Normalization	1.0000 ± 0.0025	
	Detector efficiency	-	
	Self-shielding	-	
	Time-of-flight binning	Zone length / bin width 10240 / 2 ns 4096 / 4 ns 4096 / 8 ns 4096 / 16 ns 4096 / 32 ns 4096 / 64 ns 6144 / 128 ns 28672 / 64 ns	
9.	**Response function**		
	Initial pulse	Normal distribution, FWHM = 2 ns	
	Target / moderator assembly	Numerical distribution from MC simulations	[f][g]
	Detector	Analytical function defined in REFIT manual	[h]

B. Data format

Column	Content	Unit	Comment
1	Energy	eV	Relativistic relation using a fixed flight path length (L = 10.860 m)
2	t_l	ns	Low bound
3	t_h	ns	High bound
4	T_{exp}		Transmission
5	Total Uncertainty		
6	Uncorrelated uncertainty		Uncorrelated uncertainty due to counting statistics
7	AGS-vector (K)		Background model uncertainty (u_K/K=3 %)
8	AGS-vector (N)		Normalization (u_N/N = 0.25 %)

Comments from the authors:

- The AGS concept was used to derive the experimental transmission

$$T_{exp} = N\frac{C_{in} - KB_{in}}{C_{out} - KB_{out}},$$

  and to propagate the uncertainties, both the uncorrelated due to counting statistics and the uncertainty due to the normalization and the background contributions.
- The quoted uncertainties are standard uncertainties at 1 standard deviation

B.1 DATA (ID 1)

E/ eV	t_l / ns	t_h / ns	T_{exp}	u_t	u_u	AGS K	N
120.0097	71664	71680	0.989435	0.039879	0.039802	-0.000112	0.002474
119.9562	71680	71696	0.947476	0.037403	0.037325	-0.000442	0.002369
…	…	…	…	…	…	…	…
5.401749	337792	337856	0.211735	0.009283	0.009079	-0.001862	0.000529
5.399703	337856	337920	0.218383	0.009598	0.009391	-0.001905	0.000546
…	…	…		…	…	…	…
0.400107	1241216	1241344	0.732863	0.298858	0.297676	-0.026491	0.0018
0.400024	1241344	1241472	1.002894	0.434305	0.434298	0.000367	0.002507

B.2 DATA (ID 2)

E/ eV	t_l / ns	t_h / ns	T_{exp}	u_t	AGS		
					u_u	K	N
120.0097	71664	71680	0.876494	0.218082	0.217730	-0.012191	0.002191
119.9562	71680	71696	0.961967	0.231891	0.231782	0.006587	0.002676
…	…	…	…	…	…	…	…
5.401749	337792	337856	0.218486	0.003338	0.003266	-0.000420	0.000546
5.399703	337856	337920	0.212007	0.003288	0.003217	-0.000425	0.000530
…	…	…		…	…	…	…
0.400189	1241088	1241216	1.215978	0.271888	0.271446	0.015196	0.003040
0.400107	1241216	1241344	1.122953	0.243238	0.243088	0.008064	0.002807

B.3 DATA (ID 3)

E/ eV	t_l / ns	t_h / ns	T_{exp}	u_t	AGS		
					u_u	K	N
120.0097	71664	71680	0.959551	0.038012	0.037935	-0.000329	0.002399
119.9562	71680	71696	0.961967	0.037997	0.037919	-0.000308	0.002405
…	…	…	…	…	…	…	…
5.401749	337792	337856	0.450095	0.0140702	0.013958	-0.001391	0.001125
5.399703	337856	337920	0.454635	0.014354	0.014238	-0.001414	0.001137
…	…	…		…	…	…	…
0.400107	1241216	1241344	1.050920	0.422296	0.422244	0.006101	0.002627
0.400024	1241344	1241472	1.452699	0.609102	0.605688	0.064491	0.003632

B.4 DATA (ID 4)

E/ eV	t_l / ns	t_h / ns	T_{exp}	u_t	AGS		
					u_u	K	N
120.0097	71664	71680	0.877777	0.254469	0.217730	-0.012191	0.002191
119.9562	71680	71696	0.995764	0.232403	0.232390	0.006587	0.002676
…	…	…	…	…	…	…	…
5.401749	337792	337856	0.218486	0.003338	0.003266	-0.000420	0.000546
5.399703	337856	337920	0.212007	0.003288	0.003217	-0.000425	0.000530
…	…	…		…	…	…	…
0.411140	1224448	1224576	0.373967	0.233334	0.222561	-0.070076	0.000935
0.411054	1224576	1224704	0.888347	0.352434	0.243088	-0.015208	0.002221

References

[a] L. Šalamon, B. Geslot, J. Heyse, S. Kopecky, P. Leconte, G. Noguere, C. Paradela, P. Schillebeeckx and L. Snoj, "^{107}Ag and ^{109}Ag resonance parameters for neutron induced reactions below 1 keV", Nuclear Inst. Meth. B 446 (2019) 19-28.

[b] W. Mondelaers and P. Schillebeeckx, "GELINA, a neutron time-of-flight facility for neutron data measurements", Notiziario Neutroni e Luce di Sincrotrone, 11 (2006) 19 – 25.

[c] B. Becker, C. Bastian, F. Emiliani, F. Gunsing, J. Heyse, K. Kauwenberghs, S. Kopecky, C. Lampoudis, C. Massimi, N. Otuka, P. Schillebeeckx and I. Sirakov, "Data reduction and uncertainty propagation of time-of-flight spectra with AGS", J. of Instrumentation, 7 (2012) P11002 – 19.

[d] P. Schillebeeckx, B. Becker,Y. Danon, K. Guber, H. Harada, J. Heyse, A.R. Junghans, S. Kopecky, C. Massimi, M.C. Moxon, N. Otuka, I. Sirakov and K. Volev, "Determination of resonance parameters and their covariances from neutron induced reaction cross section data", Nuclear Data Sheets 113 (2012) 3054 – 3100.

[e] B. Becker, C. Bastian, F. Emiliani, F. Gunsing, J. Heyse, K. Kauwenberghs, S. Kopecky, C. Lampoudis, C. Massimi, N. Otuka, P. Schillebeeckx and I. Sirakov, "Data reduction and uncertainty propagation of time-of-flight spectra with AGS", J. of Instrumentation, 7 (2012) P11002 – 19.

[f] M. Flaska, A. Borella, D. Lathouwers, L.C. Mihailescu, W. Mondelaers, A.J.M. Plompen, H. van Dam and T.H.J.J. van der Hagen, "Modeling of the GELINA neutron target using coupled electron–photon–neutron transport with the MCNP4C3 code", Nucl. Instr. Meth. A 531 (2004) 392–406.

[g] D. Ene, C. Borcea, S. Kopecky, W. Mondelaers, A. Negret and A.J.M. Plompen, "Global characterisation of the GELINA facility for high-resolution neutron time-of-light measurements by Monte Carlo simulations", Nucl. Instr. Meth. A 618 (2010) 54 - 68.

[h] M.C. Moxon and J.B. Brisland, Technical Report AEA-INTEC-0630, AEA Technology (1991).

Nuclear Data Section
International Atomic Energy Agency
P.O. Box 100
A-1400 Vienna
Austria

e-mail: nds.contact-point@iaea.org
fax: (43-1) 26007
telephone: (43-1) 2600 21725
Web: http://www-nds.iaea.org/